

An investigation into the cytotoxic effects of microbubbles and their constituents on osteosarcoma and bone marrow stromal cells

A.E. Polydorou^{a,b}, J.P. May^{a,b}, K. Makris^b, S. Ferri^{a,b}, Q. Wu^c, E. Stride^{c,d}, D. Carugo^d, N.D. Evans^{a,b,*}

^a Centre for Human Development, Stem Cells and Regenerative Medicine, Bone and Joint Research group, University of Southampton, United Kingdom

^b Bioengineering Sciences Group, Institute for Life Sciences, University of Southampton, United Kingdom

^c Institute of Biomedical Engineering, University of Oxford, United Kingdom

^d Botnar Research Centre, Nuffield Department of Orthopaedics, Rheumatology and Musculoskeletal Sciences (NDORMS), University of Oxford, United Kingdom

ARTICLE INFO

Keywords:

Microbubble
Toxicity
Phospholipids
Polyethylene glycol
Bone

ABSTRACT

Background: Ultrasound-responsive microbubbles offer a means of achieving minimally invasive, localised drug delivery in applications including regenerative medicine. To facilitate their use, however, it is important to determine any cytotoxic effects they or their constituents may have. The aim of this study was to test the hypothesis that phospholipid-shelled microbubbles are non-toxic to human bone-derived cells at biologically-relevant concentrations.

Methods: Microbubbles were fabricated using combinations of 1,2-distearoyl-sn-glycero-3-phosphocholine (DSPC), 1,2-dibehenoyl-sn-glycero-3-phosphocholine (DBPC), polyoxyethylene(40) stearate (PEG40S) and 1,2-distearoyl-sn-glycero-3-phosphoethanolamine-N-[methoxy(polyethylene-glycol)-2000] (DSPE-PEG₂₀₀₀). Microbubble size and concentration were measured as a function of time and temperature by optical microscopy. Effects on MG63 osteosarcoma and human bone marrow stromal cells (BMSCs) were measured for up to 72 h by assay for viability, metabolic activity and proliferation.

Results: DBPC:DSPE-PEG₂₀₀₀ microbubbles were significantly more stable than DSPC:PEG40S microbubbles under all conditions tested. Serum-containing medium had no detrimental effect on microbubble stability, but storage at 37 °C compared to at 4 °C reduced stability for both preparations, with almost complete dissolution of microbubbles at times ≥ 24 h. DSPC:PEG40S microbubbles had greater inhibitory effects on cell metabolism and growth than DBPC:DSPE-PEG₂₀₀₀ microbubbles, with PEG40S found to be the principle inhibitory component. These effects were only evident at high microbubble concentrations ($\geq 20\%$ (v/v)) or with prolonged culture (≥ 24 h). Increasing cell-microbubble contact by inversion culture in a custom-built device had no inhibitory effect on metabolism.

Conclusions: These data indicate that, over a broad range of concentrations and incubation times, DBPC:DSPE-PEG₂₀₀₀ and DSPC:PEG40S microbubbles have little effect on osteoblastic cell viability and growth, and that PEG40S is the principle inhibitory component in the formulations investigated.

1. Introduction

Microbubbles are currently used clinically as contrast agents in diagnostic ultrasound imaging. They typically comprise a surfactant shell which stabilises a core of a high molecular weight and poorly water-soluble gas, such as perfluorobutane or sulphur hexafluoride. Due to their high compressibility and the significant acoustic impedance mismatch with surrounding tissues, they scatter incident ultrasound and

produce excellent contrast between blood vessels and the surrounding tissue. Microbubbles are used in diagnosis in a range of clinical applications, including cardiovascular medicine and urology [1,2]. The same volumetric oscillations that produce acoustic scattering can also be exploited therapeutically to manipulate or perturb tissues through remote extracorporeal activation [3], for example to increase vessel permeability and to enhance site-specific delivery of circulating drugs, either attached to or co-administered with microbubbles [4–6]. Notably,

* Corresponding author at: Centre for Human Development, Stem Cells and Regenerative Medicine, Bone and Joint Research group, University of Southampton, United Kingdom.

E-mail address: n.d.evans@soton.ac.uk (N.D. Evans).

<https://doi.org/10.1016/j.bbagen.2023.130481>

Received 19 July 2023; Received in revised form 26 September 2023; Accepted 2 October 2023

Available online 5 October 2023

0304-4165/© 2023 The Authors. Published by Elsevier B.V. This is an open access article under the CC BY license (<http://creativecommons.org/licenses/by/4.0/>).

ultrasound-induced oscillation of microbubbles generates mechanical forces that can increase drug convection in a target tissue compared to passive diffusion [7]. Most applications of ultrasound-responsive microbubbles in drug delivery to date have been in the field of cancer, for example in the treatment of brain [8] and pancreatic tumours [9]. However, other applications are emerging, including but not limited to urology and infection control [10,11], thrombolysis [12], and neurodegeneration [13]. We and others [14] are exploring the notion that microbubbles may be adapted for drug delivery to enhance bone repair and regeneration.

Formulations of microbubbles are generally regarded as safe and biocompatible *in vivo*, with many formulations approved for clinical use. Several of these clinical formulations, such as SonoVue®, Definity®, and Sonazoid® have a lipid shell, with some also containing a polyethylene glycol (PEG) moiety [15]. 1,2-distearoyl-sn-glycero-3-phosphocholine (DSPC) is an example of a common constituent of clinical microbubble formulations, such as SonoVue®, and microbubbles containing DSPC have been largely researched for application in ultrasound-mediated drug delivery [10,16]. Microbubbles containing 1,2-dibehenoyl-sn-glycero-3-phosphocholine (DBPC) have also been researched for their potential in controlled delivery of biologically active gases, such as oxygen and nitric oxide [9,11]. Despite their approved clinical use, there are a number of minor and/or rare adverse reactions that have been reported in the literature (reviewed by Appis et al. [1]). For example, Definity® has been associated with back pain, hypotension and angioedema [17], SonoVue® is contraindicated in patients with hypersensitivity to formulation components and pulmonary hypertension, while Sonazoid® is associated with side effects including diarrhoea, albuminuria and neutropenia [4]. In addition, anti-PEG antibodies have been associated with enhanced clearance of microbubbles, altering their efficacy [18]. These findings highlight the importance of understanding the effect of independent microbubble components on both target cells *in-vitro* and in organisms prior to clinical development for an intended use. However, the majority of published studies focus predominantly on the effect of the active administered drug or ultrasound regimen, with less attention being paid to the effect of the microbubble formulation alone. Notably, most microbubble formulations are assumed to be safe due to the postulated biocompatibility and common usage of constituent compounds, such as DSPC and PEG40S [19]. As a result, there are very few examples of systematic studies in the literature on the effect of microbubble components on cells.

We are investigating the notion that microbubbles may have potential for applications in drug delivery in bone biology. To the best of our knowledge there are no studies that focus on evaluating the cytotoxicity of microbubbles on bone lineage cells. Therefore, in this study we aimed to test the hypothesis that phospholipid-shelled microbubbles are non-toxic to human bone-derived cells at biologically relevant concentrations and exposure times.

2. Methods

2.1. Microbubble fabrication

Two formulations of air-filled microbubbles were prepared using 9:1 M ratios either of 1,2-distearoyl-sn-glycero-3-phosphocholine (DSPC) to polyoxyethylene(40) stearate (PEG40S) (referred to as “**DSPC:PEG40S microbubbles**” hereafter), or 1,2-dibehenoyl-sn-glycero-3-phosphocholine (DBPC) to 1,2-distearoyl-sn-glycero-3-phosphoethanolamine-N-[methoxy(polyethylene glycol)-2000] (DSPE-PEG₂₀₀₀) (“**DBPC:DSPE-PEG₂₀₀₀ microbubbles**”). Lipids were purchased from Avanti Lipids and PEG40S from Sigma (Poole, UK). Lipids were dissolved in chloroform to concentrations of 25 mg/mL (phospholipids) or 10 mg/mL (PEG-containing constituents) and mixed at 9:1 for DSPC:PEG40S and DBPC:DSPE-PEG₂₀₀₀ in glass specimen vials to the same final overall lipid mass (Fisherbrand™, UK). Molar ratios between microbubble shell constituents were selected to be representative of those commonly used

in research involving similar microbubble formulations. Lipid solutions were evaporated overnight at room temperature to form dry lipid films, which could be stored at −20 °C in this form before rehydration in sterile PBS (5 mL) to form lipid suspensions at a concentration of 4 mg/mL. Samples were stirred and warmed at 90–100 °C for 30 min, above the lipids' phase-transition temperatures. To ensure thorough dispersion of lipids, samples were first sonicated for 150 s at 48 W with submersion of a 3.22 mm diameter sonicator tip (120 Sonic Dismembrator, Fisher Scientific, UK) to form lipid suspensions (LS). For microbubble (MB) fabrication, samples were then sonicated a second time for 30 s at 84 W with the sonicator tip positioned at the gas-liquid interface to encapsulate air. The formed microbubble suspensions were cooled in an ice bath for 5 min and stored at 4 °C prior to characterisation and use.

2.2. Microbubble characterisation

Microbubble suspensions were diluted 1:10 (v/v) either in PBS alone, or in Dulbecco's modified Eagle's medium (DMEM; Lonza, UK) supplemented with 10% fetal bovine serum (FBS) (Gibco, ThermoFisher, UK), and incubated at 4 or 37 °C in final volumes of 1 mL. A volume of 20 µL of each suspension was injected in a Fast-Read 102® plastic counting chamber (Sigma, UK) and, at various timepoints for up to a week, at least 10 different images of microbubbles were taken using an EVOS XL Core microscope with a × 40 magnification objective (covering the entire slide), as indicated in the Results section. The images were processed using ImageJ to calculate bubble number and dimension in pixels. Data were processed in Microsoft Excel with pixel area converted into diameter (in µm) assuming circularity of 1. Microbubble concentration was also calculated based on the measured microbubble number and sample volume.

2.3. Cell culture

MG63 cells were cultured in high-glucose DMEM supplemented with 10% (v/v) FBS and 1% (v/v) penicillin-streptomycin (Lonza, UK; containing 10,000 U/mL penicillin and streptomycin). Cells were seeded at 6,000 cells/cm² prior to the addition of any test reagent. Cells were passaged every 3–4 days at 80% confluence. Primary STRO-1⁺ selected bone marrow stromal cells were isolated from patients at Southampton General Hospital, with patients' written informed consent and approval of the local research ethics committee (LREC 194/99), as previously reported [20]. BMSCs were cultured in minimum essential medium - alpha modification (α-MEM) (Lonza, UK) containing L-glutamine and 4.5 g/L of glucose - which was supplemented with batch-tested 10% FBS (v/v) and 1% (v/v) penicillin-streptomycin containing 10,000 units/mL of penicillin and 10,000 units/mL of streptomycin (Lonza, UK). BMSCs were seeded at 10,000 cells/cm² and passaged at 70% confluence every 5–7 days.

2.4. alamarBlue™ cellular metabolic activity and PicoGreen™ cellular DNA assays

To determine the effect of microbubble formulations on metabolic activity and DNA synthesis, cells were incubated with various concentrations of microbubbles for between 20 min and 72 h. Although it has been reported that lipid-shelled microbubbles typically have a half-life in the order of minutes in the circulatory system [21], the microbubble's shell constituents are likely to persist longer, with PEG moieties for example having circulatory half-lives of hour to days [22]. Therefore, a relatively broad range of incubation timescales was investigated to account for different physical forms in which the microbubble shell constituents would be present upon administration. After incubation, wells were washed with PBS and 100 µL of 10% (v/v) solution of commercial alamarBlue™ reagent in basal media was added to each well. Cells were incubated with alamarBlue™ for 2 h. Live, metabolically active cells reduce resazurin to the fluorescently active compound,

resorufin (peak emission wavelength, $\lambda_{em} = 584$ nm), providing a fluorescent measure of whole-culture metabolic activity. Following alamarBlue™ incubation, the supernatant was aspirated and its steady-state fluorescence intensity was quantified in triplicate using a GloMax® Discover (Promega, UK) plate reader with fluorescence detected at wavelengths of 520 nm (excitation) and between 580 nm and 640 nm (emission). Following fluorescence measurement for alamarBlue™, wells were washed using PBS and 100 μ L/well of Cellytic M (Sigma, UK) was added. Cells were then stored at -20 °C until further analysis. Prior to analysis, cells were lysed by freeze/thawing prior to disruption by scraping and trituration using a 100 μ L pipette tip. The suspensions were then vortexed for 10 s and 10 μ L of each suspension from each centrifuge tube was then transferred in duplicate to 96 well plates. TRIS/EDTA buffer (90 μ L, 1% v/v) was added to all wells and 100 μ L working solution of Quant-iT™ PicoGreen was then added to each well. The plate was incubated for 5 min before measurement using GloMax ($\lambda_{ex} = 480$ nm and $\lambda_{em} = 520$ nm).

2.5. Live/dead cell staining assay

The Live/dead assay was carried out according to the manufacturer's instructions (ThermoFisher Scientific, UK). Specifically, calcein AM and ethidium homodimer-1 (ETH-1) were added to serum free α -MEM to make final concentrations of 4 mM and 2 mM, respectively. Briefly, following cell incubation in 24 well plates in the presence of microbubble concentrations of up to 50% (v/v) for up to 72 h, cells were washed with PBS and 200 μ L of the staining solution was then added to each well and incubated at room temperature for 35 min. Cells were then imaged using an Axiovert 200 inverted microscope (Zeiss, Germany) at $\times 10$ objective lens magnification with a FITC filter ($\lambda_{ex} = 494$ nm and $\lambda_{em} = 517$ nm) to image live cells stained with calcein AM, and an RFP filter ($\lambda_{ex} = 528$ nm and $\lambda_{em} = 617$ nm) for dead cells stained with ethidium homodimer. Images were processed using ImageJ software by separating individual channels, applying a different colour for each stain, and quantifying the number of cells for each colour.

2.6. Design of inverted plate for cell-microbubble contact assays

A two-part mould was fabricated using Solidworks software (Dassault Systèmes, France) to produce a replacement lid for a 24-well tissue culture plate to enable inverted, long-term culture of adherent mammalian cells. The lid design comprised a flat substrate surface with an array of inserts that would fit within commercial wells, to provide an effective sealing. The upper and lower parts of the moulds were manufactured in polylactic acid (PLA) with a fused deposition modelling 3D printer (Ultimaker S3, UK). The dimensions of a 24-well plate were used as a reference to design the lid, and each well insert was 15.9 mm long. Each insert had two inlets, 2 mm in diameter, one to inject the microbubble suspension and the other to allow displaced air to exit the well during priming. The lid was made from polydimethylsiloxane (PDMS) (DowSil Sylgard 184) by mixing PDMS monomer and curing agent, at a mass ratio of 10:1. PDMS was first poured into the lower mould halfway, then the upper mould was mated with the lower mould. The assembled mould was then filled with PDMS allowing for the spill over to be collected into the overflow. The mould was then placed into a desiccator until the PDMS was fully degassed and appeared clear. PDMS was cured for 72 h at room temperature before the mould was removed and was autoclaved prior to use for tissue culture. Upon application of the lid to a well plate, a vacuum was formed which aided the leak-proof property of the lid.

3. Results

3.1. DBPC:DSPE-PEG₂₀₀₀ are more stable than DSPC:PEG40S microbubbles

To determine stability, we imaged microbubbles in either PBS or growth medium at 4 and 37 °C by light microscopy and analysed the acquired images. At initial timepoints, there were noticeably more microbubbles formed from DBPC:DSPE-PEG₂₀₀₀ lipid mixtures compared with DSPC:PEG40S microbubbles ($4.47 \times 10^7 \pm 8.5 \times 10^5$ vs. $2.50 \times 10^6 \pm 3.4 \times 10^5$ [5]; $n = 2$ batches). In all cases, however, microbubble concentration declined with respect to time (Fig. 1). Despite this, DBPC:DSPE-PEG₂₀₀₀ microbubbles were evidently more stable than DSPC:PEG40S microbubbles in both PBS and growth medium, particularly at 4 °C with many microbubbles present 2 days following formation. It was also evident that there were increases in size of DSPC:PEG40S microbubbles, which was also true but less pronounced for DBPC:DSPE-PEG₂₀₀₀ microbubbles. For both formulations, storage at 37 °C compared to 4 °C had a negative effect on microbubble number, with no microbubbles observable under microscopy after 60 min incubation either in PBS or in medium for DSPC:PEG40S microbubbles, and a similar but less pronounced decline for DBPC:DSPE-PEG₂₀₀₀ microbubbles, where microbubbles were still observable at 2 h at 37 °C in both growth medium and PBS. However, at later time-points (24 and 72 h) there were fewer microbubbles observable when stored at 37 °C compared to 4 °C. Quantification of DBPC:DSPE-PEG₂₀₀₀ microbubble number (2 batches) indicated that the microbubble concentration was higher and the microbubble diameter was lower at later time points in growth medium compared to PBS (Supplementary Figs. 1 and 2).

Taken together, these data indicate that DBPC:DSPE-PEG₂₀₀₀ microbubbles are more stable than DSPC:PEG40S microbubbles, and that growth medium has little detrimental effect on DBPC:DSPE-PEG₂₀₀₀ microbubble stability compared to PBS, at either 4 or 37 °C.

3.2. DSPC:PEG40S and DBPC:DSPE-PEG₂₀₀₀ microbubbles do not inhibit MG63 metabolism or proliferation at most exposure times and concentrations

To determine any inhibitory effect of microbubbles on cell metabolism, MG63 cells were cultured for up to 72 h in the presence of increasing relative concentrations of microbubble formulations. Metabolic activity did not change significantly after exposure for 20 min, 40 min and 24 h (Fig. 2A and B). However, at 72 h, there was a dose-dependent decrease in metabolic activity, which was significant at the highest relative concentration (2 mg/mL lipids) for both formulations, where relative metabolic activity decreased from $100\% \pm 5\%$ to $44\% \pm 4\%$ ($p < 0.0001$) for DSPC:PEG40S microbubbles, while there was a lower decrease, from $100\% \pm 0.7\%$ to $72\% \pm 5\%$ ($p < 0.0001$), for DBPC:DSPE-PEG₂₀₀₀ microbubbles.

These effects were also evident as an inhibition in cell proliferation, measured by DNA concentration, with a significant decrease at 72 h for the highest concentration of microbubbles, for both DSPC:PEG40S microbubbles ($p < 0.0001$) and DBPC:DSPE-PEG₂₀₀₀ microbubbles ($p = 0.02$).

To determine which component of the microbubble formulation was responsible for inhibiting cell metabolism at 72 h, dispersions of each component of the formulation (DSPC, PEG40S, DBPC and DSPE-PEG₂₀₀₀) were investigated separately, at concentrations equivalent to their presence in microbubble formulations. As shown in Fig. 3, DSPE-PEG₂₀₀₀, DSPC and DBPC had no effect or minor effects on cell metabolic activity at any concentration tested. In contrast, PEG40S significantly inhibited metabolic activity at a relative concentration of 0.2 mg/mL with almost complete inhibition at the highest concentration. Note that at a lower concentration (0.008 mg/mL), there was a positive effect of PEG40S on cell metabolic activity.

The lipid suspensions of each microbubble formulation were also

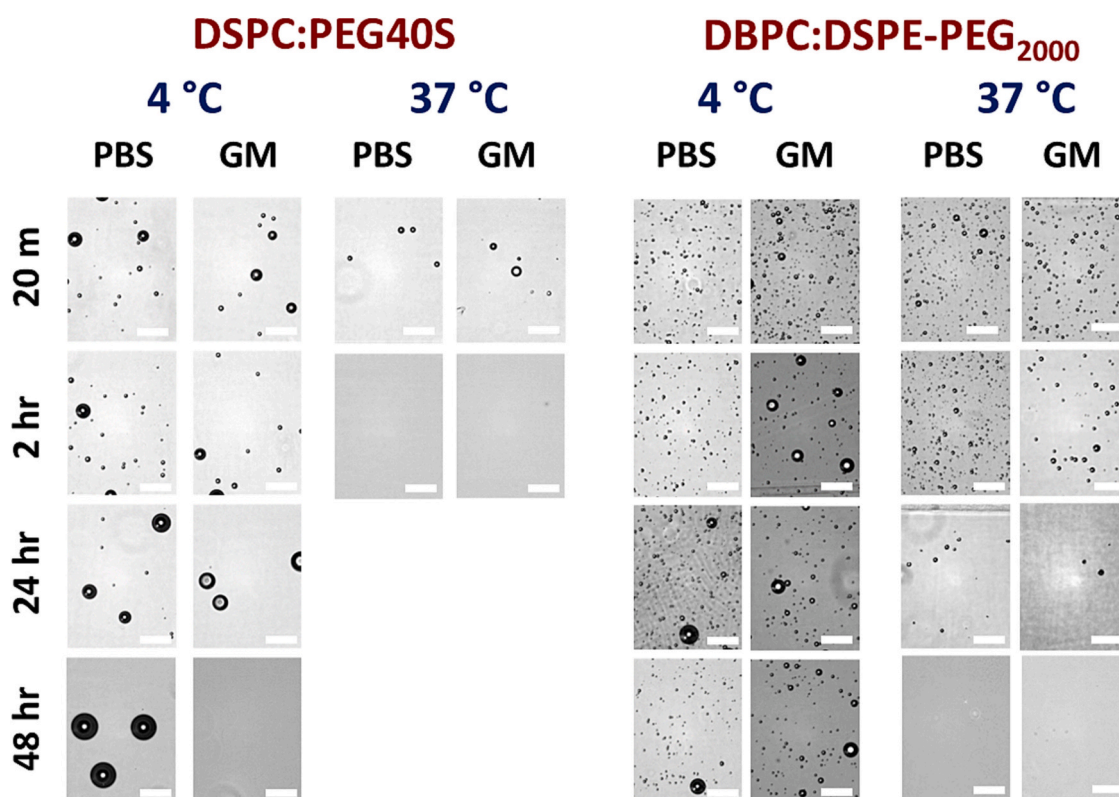


Fig. 1. DPBC:DSPE-PEG₂₀₀₀ microbubbles are more stable than DSPC:PEG40S microbubbles and increased temperature reduces microbubble stability. Change in concentration of microbubbles with respect to time at either 4 °C or 37 °C for DSPC:PEG40S or DBPC:DSPE-PEG₂₀₀₀ microbubbles diluted at 10% (v/v) (final lipid concentration 0.4 mg/mL) in PBS or growth medium (GM). Data are representative images of 10 measurements of 2 microbubble batches. Scale bars indicate 50 μm. Quantitative data can be viewed in Supplementary Fig. 1.

investigated, to evaluate whether the observed effects were due to the lipid molecules themselves and/or whether they could be fully or partly attributed to the 3-dimensional vesicular structure of the microbubble. To evaluate this, MG63 cells were incubated with DSPC:PEG40S lipid suspensions formed by sonication and compared to microbubble suspensions of the same lipid formulation. Like microbubbles, lipid suspensions at equivalent concentrations inhibited cell metabolism and cell proliferation at the two highest concentrations, but microbubbles had a significantly greater inhibitory effect than lipid dispersions alone (Supplementary Fig. 3).

Overall, these data indicate that for MG63 cells, microbubbles have inhibitory effects on cell growth and metabolism at high concentrations over prolonged periods, and this effect is in part due to PEG40S.

3.3. BMSCs are more sensitive to the inhibitory effects of DSPC:PEG40S microbubbles than MG63 cells

To determine the effect of microbubble formulations on human primary cells, we incubated both MG63 osteosarcoma cells and BMSCs with increasing concentrations of microbubble preparations and measured cell metabolic activity. As in previous experiments, both DSPC:PEG40S and DBPC:DSPE-PEG₂₀₀₀ microbubbles caused a dose-dependent inhibition of cell metabolic activity (Fig. 4A and B). In addition, for both formulations, inhibition was greater for BMSCs than for MG63 cells at all concentrations (Fig. 4B), and the inhibition induced by DSPC:PEG40S microbubbles was significantly greater than for DBPC:DSPE-PEG₂₀₀₀ for both cell types. When BMSC metabolism was studied with respect to time for high concentrations of both DSPC:PEG40S and DBPC:DSPE-PEG₂₀₀₀ microbubbles, an inhibition of metabolic activity was measured at 72 h, with a greater inhibitory effect of the former compared to the latter formulation (Fig. 4C). Finally, the greater toxic

effect of microbubbles was evident from microscopy images of cells stained with the Live/dead assay, where significant cell death was observable for DSPC:PEG40S at intermediate and high microbubble concentrations, with less of an effect for DBPC:DSPE-PEG₂₀₀₀ microbubbles (Fig. 4D).

These data support that DBPC:DSPE-PEG₂₀₀₀ are less toxic than DSPC:PEG40S microbubbles in primary human BMSC populations.

3.4. Cell-microbubble contact is not the principal cause of the inhibitory effect of microbubbles

One of the challenges in testing the effect of microbubbles on cell behaviour in culture is that microbubbles are buoyant, and therefore unlikely to contact cells in traditional cell culture plastic-ware unless actively targeted to the cell membrane. To determine the effect of microbubble contact on cells, a custom 24-well plate lid was designed and fabricated, as described in the Methods section. The design is shown in Fig. 5A and B, which allowed inversion and prolonged inverted culture of both MG63 and BMSCs with incubation of microbubble formulations in a 24 well plate. As shown in Fig. 5C and D, there was no significant effect on BMSC cell metabolic activity by inversion in the absence of microbubbles during a 20-min incubation. However, both DSPC:PEG40S and DBPC:DSPE-PEG₂₀₀₀ microbubbles caused reductions in cell metabolic activity at the highest concentration ($p < 0.01$) when the plate was not inverted, compared to inverted groups. This indicates that at this time point (20 min), microbubble contact does not directly affect cell metabolic activity, and that deposition of denser microbubble constituents may be responsible for the inhibition of cell metabolic activity and cell proliferation observed.

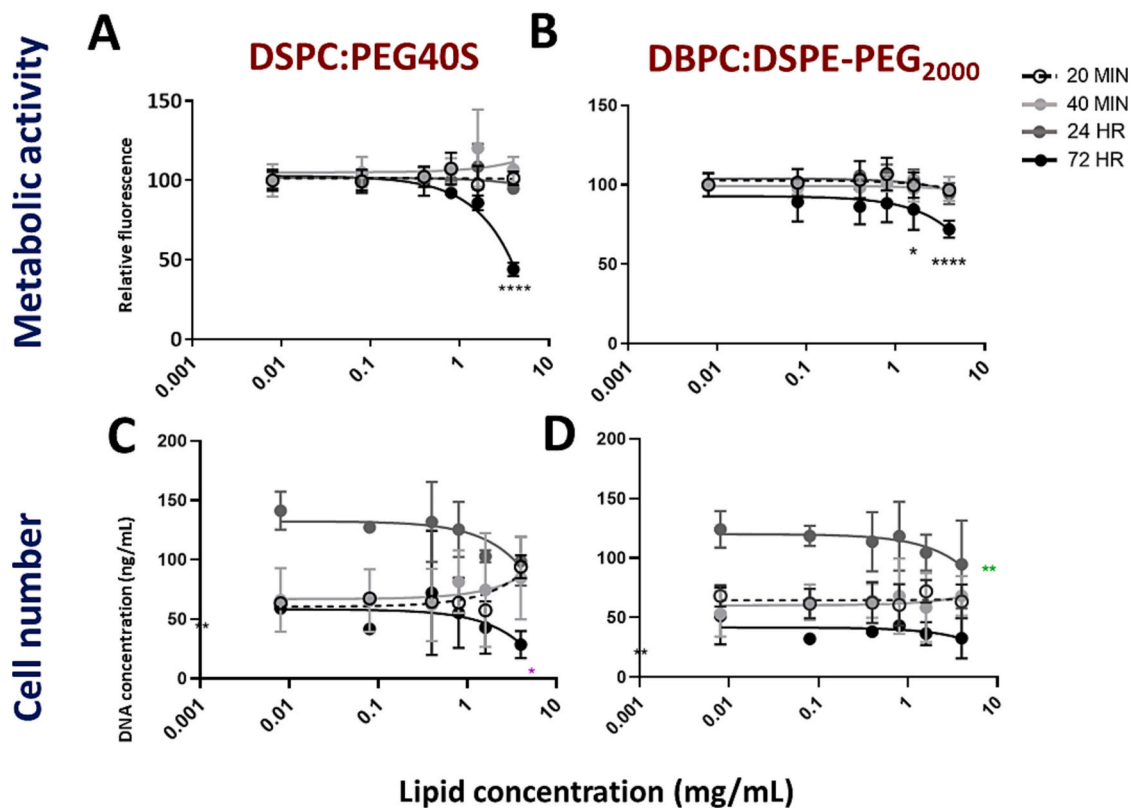


Fig. 2. DSPC:PEG40S and DBPC:DSPE-PEG₂₀₀₀ MBs have a dose and time dependent inhibitory effect on MG63 cell metabolism and proliferation. DSPC:PEG40S (A) and DBPC:DSPE-PEG₂₀₀₀ (B) microbubbles significantly reduced relative metabolic activity at 72 h, at a lipid concentration of 2 mg/mL (**** = $p < 0.0001$). At this same concentration, DSPC:PEG40S significantly reduced DNA concentration at 72 h vs. vehicle control (*; $p = 0.02$) (C), while for DBPC:DSPE-PEG₂₀₀₀ microbubbles there was a small but significant inhibitory effect on DNA concentration at 24 h (**; $p = 0.002$) (D). Two experimental repeats on separate batches were carried out in triplicate.

4. Discussion

This study aimed to determine the toxicity of lipid-coated microbubbles and their constituents, for application in orthopaedic medicine by measuring their effects on continuous and primary osteoblastic cell strains. Given the wide and growing application of lipid carriers and the potential of microbubbles as drug delivery agents, determining their likely toxicity in relevant applications is a necessary step. As described earlier, two model microbubble formulations were selected in the present study, DSPC:PEG40S and DBPC:DSPE-PEG₂₀₀₀, which are widely employed in previous literature reporting on therapeutic applications of microbubbles. Moreover, DSPC and PEG-moieties are often present in clinically approved formulations of microbubble contrast agents. Findings from this study demonstrated firstly that DBPC:DSPE-PEG₂₀₀₀ microbubbles are more stable than DSPC:PEG40S, and secondly that serum-containing medium does not negatively affect the stability of either formulation. Furthermore, both formulations negatively impacted cell metabolism and growth only at either high concentrations or longer time exposures (>24 h), with DBPC:DSPE-PEG₂₀₀₀ microbubbles having a lower negative impact compared to DSPC:PEG40S microbubbles. In addition, PEG40S was found to be responsible for the majority of the observed inhibitory effects on metabolism and proliferation, and microbubble-cell contact was not likely to be the primary mechanism of inhibition.

It is well established that the improved stability of DBPC-containing microbubbles compared to those containing other commonly used lipids, such as DSPC or DPPC, is likely due to the longer lipid acyl chain length of DBPC compared to DSPC (22 vs. 18 carbon chain). This feature has been shown to allow microbubbles to withstand greater mechanical forces as well as slow down the rate of gas diffusion, due to stronger van

der Waals interactions which help maintain microbubble stability [23–26]. The type of PEG moiety employed may also impact on microbubble stability, as PEG is known to play a role in preventing microbubble coalescence, reducing surface tension, and reducing surface adsorption of proteins present in the surrounding medium [27]. For example, in previous work, Owen et al. showed that at room temperature, DSPC:DSPE-PEG₂₀₀₀ microbubbles were more stable than DSPC:PEG40S microbubbles [28], which is also consistent with the greater stability of microbubbles incorporating DSPE-PEG₂₀₀₀ in this study.

Ensuring stability at physiological temperatures as well as in storage conditions is critical for clinical translation. Our observation that stability was reduced for both formulations at 37 °C compared to 4 °C is supported by other studies. For example, SonoVue® microbubble stability decreases with increasing temperature [29,30], an observation that has also been made with other formulations [31]. Interestingly, we did not observe any significant difference in stability between microbubbles diluted in PBS and those diluted in serum-containing growth medium. This is surprising as other studies have measured reduced microbubble stability in serum-containing medium [28], which is thought to be via binding of serum proteins to the microbubble shell, leading to compromised shell integrity or aggregation and coalescence. These results may suggest, however, that the formulation-specific PEG moieties used in the present study are effective at reducing incorporation of proteins present in cell medium into lipid-shelled microbubbles, reducing coalescence and improving stability.

In cell culture experiments, it was notable that for exposure periods during which microbubbles were found to be stable in serum-containing medium (<24 h), there were no significant effects on either osteoblastic cell metabolism or cell proliferation. The only significant inhibitory effects on both MG63 cells and BMSCs were for incubation periods of 24 h

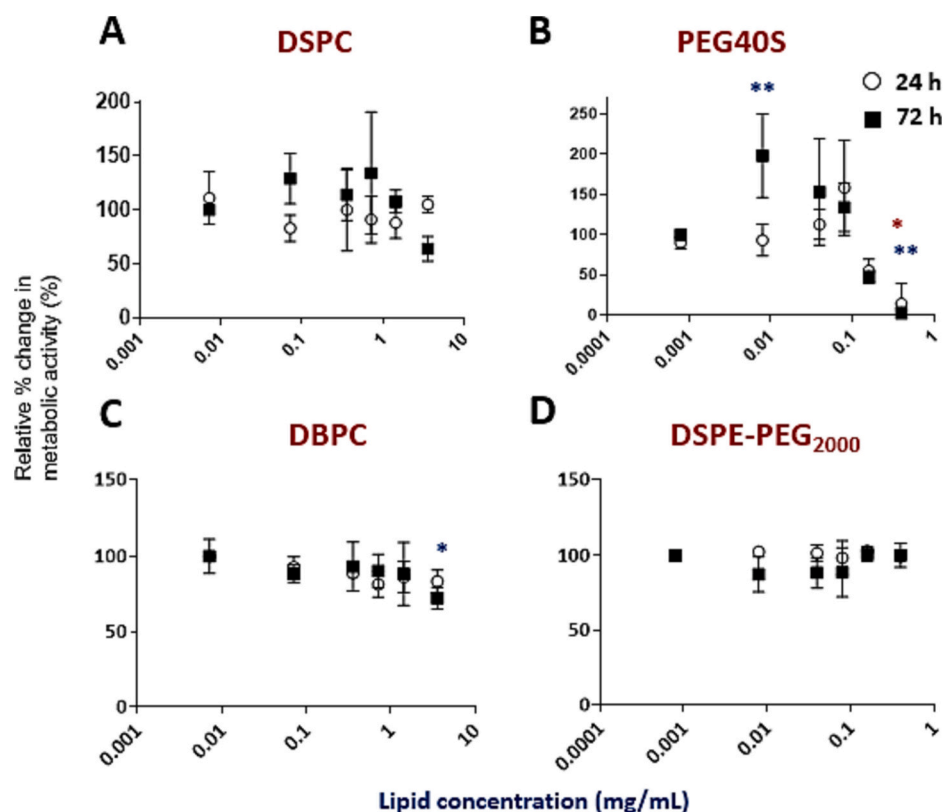


Fig. 3. PEG40S has an inhibitory effect on cell metabolism. At equivalent concentrations of microbubble formulations, DSPC has no significant effect on cell metabolism at 24 or 72 h (A), PEG40S has a significant inhibitory effect at the highest concentration and a small positive effect at the lowest concentration (B), DBPC has a small inhibitory effect at 72 h at the highest concentration (C), and DSPE-PEG₂₀₀₀ has no inhibitory effect (D). Coloured asterisk denotes significant differences assessed by ANOVA, of each treatment compared to the control (* = $p < 0.05$, ** = $p < 0.005$).

or greater, at very high microbubble concentrations (>20% by volume). In addition, it was found that the DSPC:PEG40S formulations had a greater inhibitory effect than the DBPC:DSPE-PEG₂₀₀₀ formulations, and that the only component that had a significant inhibitory effect when tested separately was PEG40S. This, combined with our data suggesting that cell contact has no measurable effect on cell metabolism (by plate inversion), indicates that shell components that are released in the medium upon microbubble degradation may induce toxic or inhibitory effects on cells, rather than microbubble contact *per se*. The exact form of these products of microbubble degradation is not fully clear, but they likely comprise of supramolecular aggregates (*i.e.* vesicular and micellar systems). Plate inversion may have reduced the interaction between microbubble degradation products and cells, which would support the lack of measurable effects in this specific group of experiments. Despite this possibility, it has been found that microbubble formulations produced by sonication methods comprise a very high fraction of unincorporated lipids (for example in micelles) [32], which indicates that it is unlikely the presence of lipids *per se* that causes the inhibitory effect. In addition, we found that lipid dispersions caused a lower inhibitory effect when compared to microbubbles, which suggests that prior formation of microbubbles is necessary for the toxic effect of the degradation products that are subsequently formed. This puzzling discrepancy may relate to differences in the production methodology – lipid dispersions were formed by sonication of bulk solutions, whereas to produce microbubbles an additional sonication step at the air-liquid interface was performed. It is possible that in the case of lipid dispersions, there is a lower free lipid or micellar concentration available to cells, with more lipids present in larger aggregates, and that it is the former configuration of lipids that induces the observed inhibitory effects. Further studies to better assess the chemical and physical composition of the medium will be necessary to test this hypothesis.

The finding that DSPC:PEG40S microbubbles disassemble more quickly than DBPC:DSPE-PEG₂₀₀₀ microbubbles, and contain a component (*i.e.* PEG40S) that is more toxic than in the latter formulation, indicate that it may be a faster disassembly rate combined with the presence of a more inhibitory component that make DSPC:PEG40S microbubbles more detrimental to cells than DBPC:DSPE-PEG₂₀₀₀. These observations may also suggest that PEG40S incorporates more easily into cell membrane bilayers compared to DSPE-PEG₂₀₀₀.

There are limited published data available on the relative contributions of microbubbles or their components on cell metabolic activity, viability or growth. One component, PEG40S, has been studied together with a large range of other PEGylated surfactants for use in cosmetic products and they have been found to be largely well tolerated [33,34], and have minimal toxicity in a number of cell lines [35]. Nevertheless, we could not find evidence in the literature that effects of PEGylated stearate or other fatty acids have been studied systematically in mammalian cell culture models. However, there is evidence that PEGylated fatty acids affect leukocyte locomotion [36], and PEG40S specifically has been found to inhibit cytochrome enzymes and P-glycoprotein transporters in different cell models [37], which may explain our data on inhibition of cell metabolism. Notably, PEG40S, DSPE-PEG₂₀₀₀, and indeed other modified phospholipids, are surfactants. It is likely that they may cause increase in cell membrane permeability when present at high concentrations as microbubble degradation products, which can also lead to inhibition of cell metabolism and growth. Although not used in the current studies, PEG itself has been found to have small but significant cytotoxic effects in different cell lines, including HeLa and L929 cells [38]. The lack of inhibition of cell metabolism with DSPE-PEG₂₀₀₀ in the current study, however, indicates that this may not be the case in the cell lines studied here.

Finally, the observation that BMSCs were more sensitive to the toxic

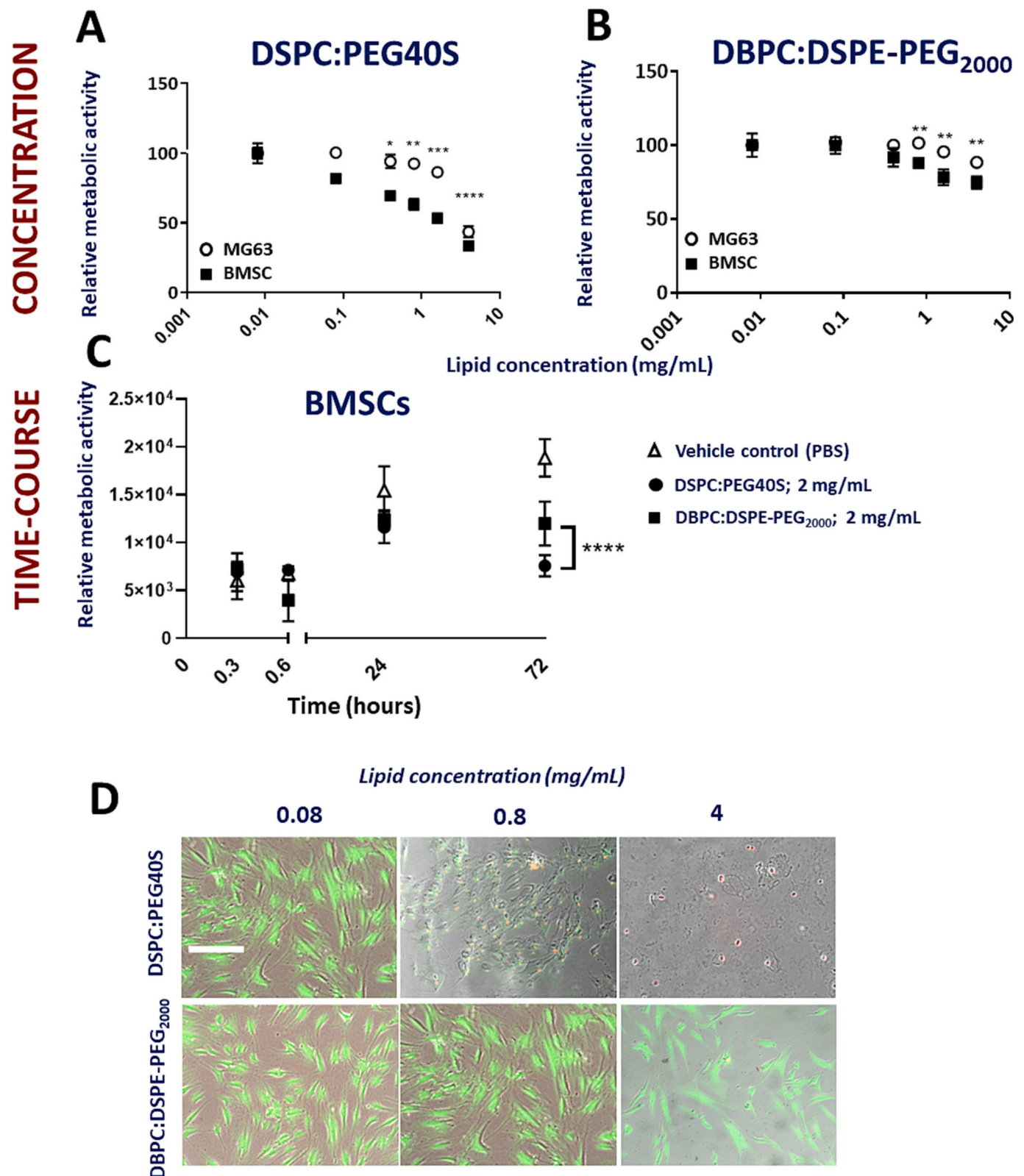


Fig. 4. DSPC:PEG40S microbubbles induce a greater dose-dependent inhibition of cell metabolism in BMSCs compared to DBPC:DSPE-PEG₂₀₀₀ microbubbles. (A) DSPC:PEG40S microbubbles inhibit cell metabolism in BMSCs to a significantly greater level than MG63 cells at all concentrations (at 72 h) except for the highest (*: $p < 0.05$; **: $p < 0.005$; ***: $p < 0.001$; ****: $p < 0.0001$). (B) In contrast, there was no significant difference in metabolic activity between MG63 and BMSCs for DBPC:DSPE-PEG₂₀₀₀ microbubbles, except for at a dilution factor of 0.01, where metabolic activity was higher in BMSCs compared to MG63s. (C) The decline in metabolic activity was also evident with respect to time, with both preparations inducing inhibition at 72 h compared to vehicle control, with a greater effect for DSPC:PEG40S microbubbles compared to DBPC:DSPE-PEG₂₀₀₀ microbubbles. (D) This was also reflected in higher cell death in cells incubated with the former compared to the latter formulation, as measured by Live/Dead staining.

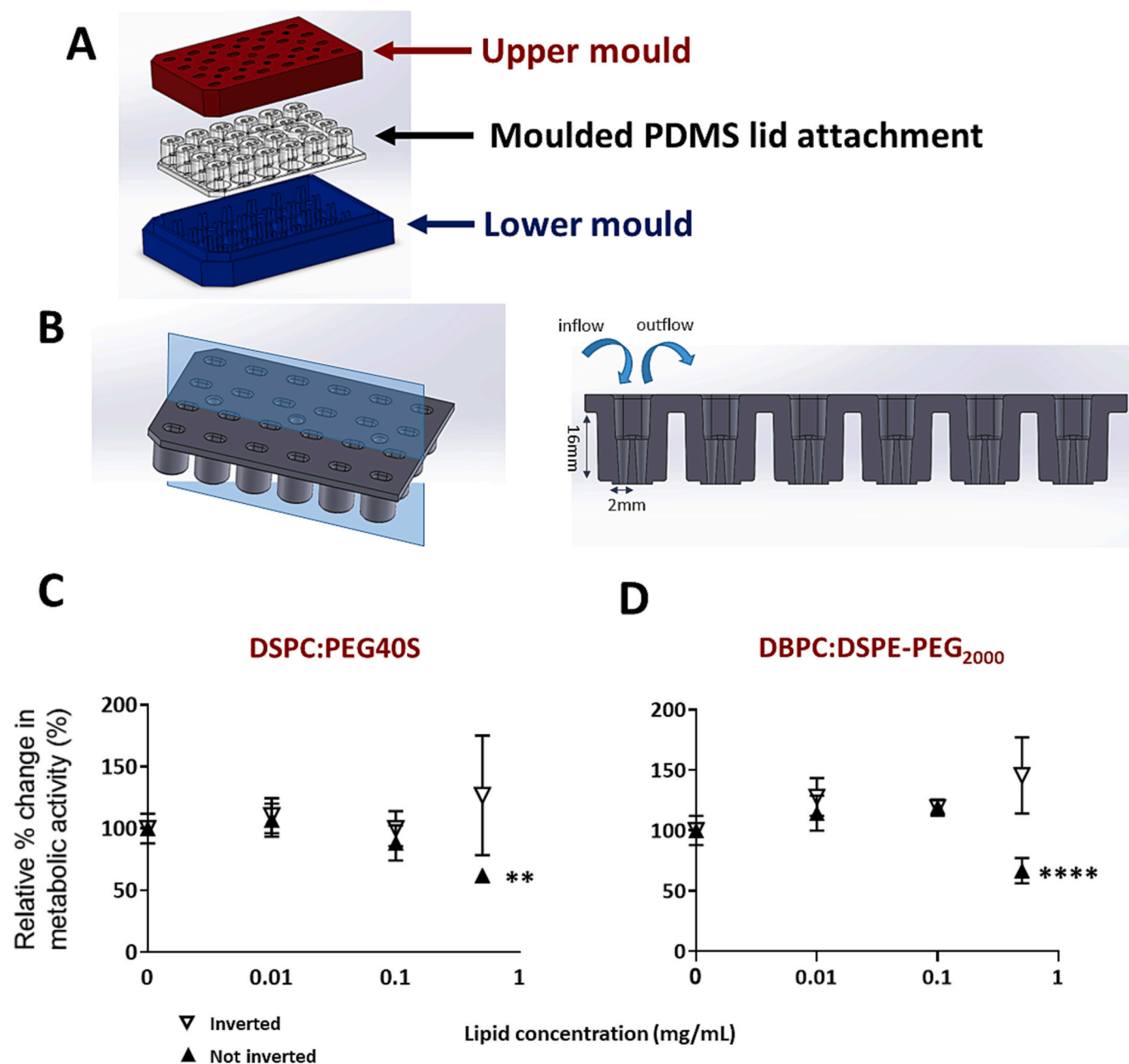


Fig. 5. Inverted plate design and absence of inhibition of metabolic activity with cell contact. (A) A mould device was designed in Solidworks comprising an upper part (red) and a lower part (blue) which - when fitted together - create a cavity where liquid PDMS was cured to form a solid plate lid (clear). (B) The lid is shown in 3D projection (left) and in cross-section (right), incorporating sealable inlet and outlet ports for priming each chamber when attached to a 24-well plate. Cell metabolism of BMSCs was significantly reduced in conventional (non-inverted culture) for both DSPC:PEG40S (C) and DBPC:DSPE-PEG₂₀₀₀ microbubbles (D) (**: $p < 0.01$; ****: $p < 0.0001$). (For interpretation of the references to colour in this figure legend, the reader is referred to the web version of this article.)

effects of microbubbles than MG63 cells, is likely due to the latter cells being osteosarcoma-derived. Cancer cell lines are well known to be more resistant to cytotoxic drugs than primary cells, and MG63 cells express a range of genes that confer drug resistance [39]. It is therefore likely that MG63 cells have general mechanisms that enable them to survive and proliferate in metabolically sub-optimal conditions, as may be the case at higher concentrations of lipid components.

In conclusion, we have tested two phospholipid-shelled microbubble formulations for their cytocompatibility with both primary and continuous bone cell strains. Our data indicate toxic effects only at prolonged exposure times or high microbubble concentrations, an effect that is likely due to degradation products of microbubbles accumulating *in vitro*. These results pave the way for future studies on the use of

ultrasound-activated microbubbles in orthopaedic medicine.

Supplementary data to this article can be found online at <https://doi.org/10.1016/j.bbagen.2023.130481>.

Credit author statement

AEP, JPM, SF, and DC conducted experiments, developed experimental protocols and interpreted and analysed data. KM developed experimental protocols and software analysis. NDE, ES and DC conceived the ideas, initiated the project, and analysed and interpreted the data. NDE and AP prepared the manuscript, with contributions from all authors. NDE, ES and DC revised the manuscript.

Declaration of Competing Interest

The authors declare the following financial interests/personal relationships which may be considered as potential competing interests: Nicholas Evans reports financial support was provided by Engineering and Physical Sciences Research Council. Anastasia Polydorou reports financial support was provided by Engineering and Physical Sciences Research Council. Jonathan May reports financial support was provided by Engineering and Physical Sciences Research Council. Sara Ferri reports financial support was provided by Engineering and Physical Sciences Research Council. Qiang Wu reports financial support was provided by Engineering and Physical Sciences Research Council. Eleanor Stride reports financial support was provided by Engineering and Physical Sciences Research Council. Dario Carugo reports financial support was provided by Engineering and Physical Sciences Research Council.

Data availability

Data will be made available on request.

Acknowledgements

The authors are grateful for funding support from the EPSRC (EPSRC EP/R013594/1 and EP/R013624/1). We acknowledge the expertise and kind help of David Chatelet for assistance with image analysis.

References

- [1] A.W. Appis, M.J. Tracy, S.B. Feinstein, Update on the safety and efficacy of commercial ultrasound contrast agents in cardiac applications, *Echo Res. Pract.* 2 (2) (2015) R55–R62, <https://doi.org/10.1530/ERP-15-0018>.
- [2] M. Versluis, E. Stride, G. Lajoie, B. Dollet, T. Segers, Ultrasound contrast agent modeling: a review, *Ultrasound Med. Biol.* 46 (9) (2020) 2117–2144, <https://doi.org/10.1016/j.ultrasmedbio.2020.04.014>.
- [3] R.E. Apfel, C.K. Holland, Gauging the likelihood of cavitation from short-pulse, low-duty cycle diagnostic ultrasound, *Ultrasound Med. Biol.* 17 (2) (1991) 179–185, [https://doi.org/10.1016/0301-5629\(91\)90125-G](https://doi.org/10.1016/0301-5629(91)90125-G).
- [4] S. Snipstad, E. Sulheim, C. de Lange Davies, C. Moonen, G. Storm, F. Kiessling, R. Schmid, T. Lammers, Sonopermeation to improve drug delivery to tumors: from fundamental understanding to clinical translation, *Expert Opin. Drug Deliv.* 15 (12) (2018) 1249–1261, <https://doi.org/10.1080/17425247.2018.1547279>.
- [5] E. Stride, T. Segers, G. Lajoie, S. Cherkaoui, T. Bettinger, M. Versluis, M. Borden, Microbubble agents: new directions, *Ultrasound Med. Biol.* 46 (6) (2020) 1326–1343, <https://doi.org/10.1016/j.ultrasmedbio.2020.01.027>.
- [6] N.Y. Rapoport, A.M. Kennedy, J.E. Shea, C.L. Scaife, K.-H. Nam, Controlled and targeted tumor chemotherapy by ultrasound-activated nanoemulsions/microbubbles, *J. Control. Release* 138 (3) (2009) 268–276, <https://doi.org/10.1016/j.jconrel.2009.05.026>.
- [7] K. Kooiman, S. Roovers, S. Langeveld, R. Kleven, H. Dewitte, M.A. O'Reilly, J. Escoffe, A. Bouakaz, M.D. Verweij, K. Hynynen, I. Lentacker, E. Stride, C. K. Holland, Ultrasound-Responsive Cavitation Nuclei for Therapy and Drug Delivery, *Ultrasound Med. Biol.* 46 (6) (2020) 1296–1325.
- [8] C.-H. Fan, C.-Y. Ting, H.-L. Liu, C.-Y. Huang, H.-Y. Hsieh, T.-C. Yen, K.-C. Wei, C.-K. Yeh, Antiangiogenic-targeting drug-loaded microbubbles combined with focused ultrasound for glioma treatment, *Biomaterials* 34 (8) (2013) 2142–2155, <https://doi.org/10.1016/j.biomaterials.2012.11.048>.
- [9] C. McEwan, S. Kamila, J. Owen, H. Nesbitt, B. Callan, M. Borden, N. Nomikou, R. A. Hamoudi, M.A. Taylor, E. Stride, A.P. McHale, J.F. Callan, Combined Sonodynamic and antimetabolite therapy for the improved treatment of pancreatic cancer using oxygen loaded microbubbles as a delivery vehicle, *Biomaterials* 80 (2016) 20–32, <https://doi.org/10.1016/j.biomaterials.2015.11.033>.
- [10] H. Horsley, J. Owen, R. Browning, D. Carugo, J. Malone-Lee, E. Stride, J.L. Rohn, Ultrasound-activated microbubbles as a novel intracellular drug delivery system for urinary tract infection, *J. Control. Release Off. J. Control. Release Soc.* 301 (2019) 166–175, <https://doi.org/10.1016/j.jconrel.2019.03.017>.
- [11] G. LuTheryn, C. Hind, C. Campbell, A. Crowther, Q. Wu, S.B. Keller, P. Glynn-Jones, J.M. Sutton, J.S. Webb, M. Gray, S.A. Wilks, E. Stride, D. Carugo, Bactericidal and anti-biofilm effects of uncharged and cationic ultrasound-responsive nitric oxide microbubbles on *Pseudomonas aeruginosa* biofilms, *Front. Cell. Infect. Microbiol.* 12 (2022) 956808, <https://doi.org/10.3389/fcimb.2022.956808>.
- [12] F. Xie, J. Lof, C. Everbach, A. He, R.M. Bennett, T. Matsunaga, J. Johanning, T. R. Porter, Treatment of acute intravascular thrombi with diagnostic ultrasound and intravenous microbubbles, *JACC Cardiovasc. Imaging* 2 (4) (2009) 511–518, <https://doi.org/10.1016/j.jcmg.2009.02.002>.
- [13] J.M. Wasieleska, J.C.S. Chaves, R.L. Johnston, L.A. Milton, D. Hernández, L. Chen, J. Song, W. Lee, G. Leinenga, R.M. Nisbet, A. Pébay, J. Götz, A.R. White, L. E. Oikari, A sporadic Alzheimer's blood-brain barrier model for developing ultrasound-mediated delivery of aducanumab and anti-tau antibodies, *Theranostics* 12 (16) (2022) 6826–6847, <https://doi.org/10.7150/thno.72685>.
- [14] M. Bez, D. Sheyn, W. Tawackoli, P. Avalos, G. Shapiro, J.C. Giacon, X. Da, S. Ben David, J. Gavriy, H.A. Awad, H.W. Bae, E.J. Ley, T.J. Kremen, Z. Gazit, K. W. Ferrara, G. Pelled, D. Gazit, In situ bone tissue engineering via ultrasound-mediated gene delivery to endogenous progenitor cells in mini-Pigs, *Sci. Transl. Med.* 9 (390) (2017), <https://doi.org/10.1126/scitranslmed.aal3128>.
- [15] F. Ja'afar, C.H. Leow, V. Garbin, C.A. Sennoga, M.-X. Tang, J.M. Seddon, Surface charge measurement of SonoVue, definity and optison: a comparison of laser doppler electrophoresis and micro-electrophoresis, *Ultrasound Med. Biol.* 41 (11) (2015) 2990–3000, <https://doi.org/10.1016/j.ultrasmedbio.2015.07.001>.
- [16] J.J. Rychak, A.L. Klivanov, Nucleic acid delivery with microbubbles and ultrasound, *Adv. Drug Deliv. Rev.* 72 (2014) 82–93, <https://doi.org/10.1016/j.addr.2014.01.009>.
- [17] C.A. Herzog, Incidence of adverse events associated with use of perflutren contrast agents for echocardiography, *JAMA* 299 (17) (2008) 2023–2025, <https://doi.org/10.1001/jama.299.17.2023>.
- [18] S.M. Fix, A.G. Nyankima, M.D. McSweeney, J.K. Tsuruta, S.K. Lai, P.A. Dayton, Accelerated clearance of ultrasound contrast agents containing polyethylene glycol is associated with the generation of anti-polyethylene glycol antibodies, *Ultrasound Med. Biol.* 44 (6) (2018) 1266–1280, <https://doi.org/10.1016/j.ultrasmedbio.2018.02.006>.
- [19] E. Stride, N. Saffari, Microbubble ultrasound contrast agents: a review, *Proc. Inst. Mech. Eng. [H]* 217 (6) (2003) 429–447, <https://doi.org/10.1243/09544110360729072>.
- [20] D. Gothard, J. Greenhough, E. Ralph, R.O. Oreffo, Prospective isolation of human bone marrow stromal cell subsets: a comparative study between Stro-1-, CD146- and CD105-enriched populations, *J. Tissue Eng.* 5 (2014), <https://doi.org/10.1177/2041731414551763>, 2041731414551763.
- [21] S.-K. Wu, P.-C. Chu, W.-Y. Chai, S.-T. Kang, C.-H. Tsai, C.-H. Fan, C.-K. Yeh, H.-L. Liu, Characterization of different microbubbles in assisting focused ultrasound-induced blood-brain barrier opening, *Sci. Rep.* 7 (2017) 46689, <https://doi.org/10.1038/srep46689>.
- [22] L. Yin, Y. Pang, L. Shan, J. Gu, The in vivo pharmacokinetics of block copolymers containing polyethylene glycol used in nanocarrier drug delivery systems, *Drug Metab. Dispos.* 50 (6) (2022) 827–836, <https://doi.org/10.1124/dmd.121.000568>.
- [23] M.A. Borden, G. Pu, G.J. Runner, M.L. Longo, Surface phase behavior and microstructure of lipid/PEG-emulsifier monolayer-coated microbubbles, *Colloids Surf. B: Biointerfaces* 35 (3–4) (2004) 209–223, <https://doi.org/10.1016/j.colsurfb.2004.03.007>.
- [24] D.H. Kim, M.J. Costello, P.B. Duncan, D. Needham, Mechanical properties and microstructure of polycrystalline phospholipid monolayer shells: novel solid microparticles, *Langmuir* 19 (20) (2003) 8455–8466, <https://doi.org/10.1021/la034779c>.
- [25] M.A. Borden, D.E. Kruse, C.F. Caskey, S. Zhao, P.A. Dayton, K.W. Ferrara, Influence of lipid shell physicochemical properties on ultrasound-induced microbubble destruction, *IEEE Trans. Ultrason. Ferroelectr. Freq. Control* 52 (11) (2005) 1992–2002.
- [26] S. Garg, A.A. Thomas, M.A. Borden, The effect of lipid monolayer in-plane rigidity on in vivo microbubble circulation persistence, *Biomaterials* 34 (28) (2013) 6862–6870, <https://doi.org/10.1016/j.biomaterials.2013.05.053>.
- [27] M.A. Borden, M.L. Longo, Dissolution behavior of lipid monolayer-coated, air-filled microbubbles: effect of lipid hydrophobic chain length, *Langmuir* 18 (24) (2002) 9225–9233, <https://doi.org/10.1021/la026082h>.
- [28] J. Owen, S. Kamila, S. Shrivastava, D. Carugo, J. Bernardino de la Serna, C. Mannaris, V. Pereno, R. Browning, E. Beguin, A.P. McHale, J.F. Callan, E. Stride, The role of PEG-40-stearate in the production, morphology, and stability of microbubbles, *Langmuir* 35 (31) (2019) 10014–10024, <https://doi.org/10.1021/acs.langmuir.8b02516>.
- [29] H. Mulvana, E. Stride, J.V. Hajnal, R.J. Eckersley, Temperature dependent behavior of ultrasound contrast agents, *Ultrasound Med. Biol.* 36 (6) (2010) 925–934, <https://doi.org/10.1016/j.ultrasmedbio.2010.03.003>.
- [30] C. Guio, G. Pastore, M. Napoleone, P. Gabriele, M. Trotta, R. Cavalli, Thermal response of contrast agent microbubbles: preliminary results from physicochemical and US-imaging characterization, *Ultrasonics* 44 (Suppl. 1) (2006) e127–e130, <https://doi.org/10.1016/j.ultras.2006.06.031>.
- [31] T. Segers, A. Lassus, P. Bussat, E. Gaud, P. Frinking, Improved coalescence stability of monodisperse phospholipid-coated microbubbles formed by flow-focusing at elevated temperatures, *Lab Chip* 19 (1) (2019) 158–167, <https://doi.org/10.1039/C8LC00886H>.
- [32] S. Unnikrishnan, Z. Du, G.B. Diakova, A.L. Klivanov, Formation of microbubbles for targeted ultrasound contrast imaging: practical translation considerations, *Langmuir* 35 (31) (2019) 10034–10041, <https://doi.org/10.1021/acs.langmuir.8b03551>.
- [33] 2 Final Report on the Safety Assessment of PEG-2, 6, 8, 12, 20, 32, 40, 50, 100, and 150 Stearates, *J. Am. Coll. Toxicol.* 2 (7) (1983) 17–34, <https://doi.org/10.3109/10915818309142000>.
- [34] C. Fruijter-Pöllth, Safety assessment on polyethylene glycols (PEGs) and their derivatives as used in cosmetic products, *Toxicology* 214 (1) (2005) 1–38, <https://doi.org/10.1016/j.tox.2005.06.001>.
- [35] H. Rachmawati, M.A. Novel, S. Ayu, G. Berlian, O.M. Tandrasmita, R. R. Tjandrawinata, K. Anggadiredja, The in vitro–in vivo safety confirmation of

- PEG-40 hydrogenated castor oil as a surfactant for oral nanoemulsion formulation, *Sci. Pharm.* 85 (2) (2017) 18, <https://doi.org/10.3390/scipharm85020018>.
- [36] C. Dahlgren, I. Rundqvist, O. Stendahl, K.-E. Magnusson, Modulation of polymorphonuclear leukocyte locomotion by synthetic amphiphiles, *Cell Biophys.* 2 (3) (1980) 253–267, <https://doi.org/10.1007/BF02790453>.
- [37] S. Zhu, R. Huang, M. Hong, Y. Jiang, Z. Hu, C. Liu, Y. Pei, Effects of polyoxyethylene (40) stearate on the activity of P-glycoprotein and cytochrome P450, *Eur. J. Pharm. Sci.* 37 (5) (2009) 573–580, <https://doi.org/10.1016/j.ejps.2009.05.001>.
- [38] G. Liu, Y. Li, L. Yang, Y. Wei, X. Wang, Z. Wang, L. Tao, Cytotoxicity study of polyethylene glycol derivatives, *RSC Adv.* 7 (30) (2017) 18252–18259, <https://doi.org/10.1039/C7RA00861A>.
- [39] C.M. Hattinger, M.P. Patrizio, L. Fantoni, C. Casotti, C. Riganti, M. Serra, Drug resistance in osteosarcoma: emerging biomarkers, therapeutic targets and treatment strategies, *Cancers* 13 (12) (2021) 2878, <https://doi.org/10.3390/cancers13122878>.